ELSEVIER

Precambrian Research 111 (2001) 31–55

Precambrian Research

www.elsevier.com/locate/precamres

Early Mesoproterozoic intrusive breccias in Yukon, Canada: the role of hydrothermal systems in reconstructions of North America and Australia

Derek J. Thorkelson [a,*], James K. Mortensen [b], Garry J. Davidson [c], Robert A. Creaser [d], Waldo A. Perez [d], J. Grant Abbott [e]

[a] *Earth Sciences, Simon Fraser University, Burnaby, BC, Canada V5A 1S6*
[b] *Earth and Ocean Sciences, University of British Columbia, Vancouver, BC, Canada V6T 2B4*
[c] *Centre for Ore Deposit Research, University of Tasmania, GPO Box 252-79, Hobart, Tasmania, Australia, 7001*
[d] *Earth and Atmospheric Sciences, University of Alberta, Edmonton, Alta., Canada, T6G 2E3*
[e] *Yukon Geology Program, Whitehorse, Yukon, Canada, Y1A 2C6*

Received 28 May 1999; accepted 24 January 2000

Abstract

In northern Yukon, Canada, numerous breccia zones of early Mesoproterozoic age (ca. 1.6 Ga) are targets for mineral exploration. Collectively termed Wernecke Breccia, they are characterized by disseminated specular hematite and local enrichment of Cu, Co, U and Au. The breccias are hosted mainly by the Paleoproterozoic Wernecke Supergroup, a 13-km thick basinal to platformal succession of carbonate and fine-grained clastic rocks. Brecciation occurred after the Wernecke Supergroup was fully lithified, deformed, and locally metamorphosed.

The breccia zones were generated by forceful explosions of volatile-rich fluids within the crust. The source of the fluids is uncertain, but may be related to igneous intrusions at depth. Rapid expansion of the fluids shattered large volumes of country rock, mainly sedimentary rocks of the Wernecke Supergroup, and dioritic to syenitic rocks of the Bonnet Plume River intrusions. In the central parts of the breccia zones, fragments underwent considerable motion, and in some cases became rounded from abrasion. Venting of brecciated rock and fluid is considered likely, but surface deposits are nowhere preserved. At one locality, large blocks of country rock foundered into open space near the top of a breccia zone, forming a fallback megabreccia. Faulting may have been active concurrently with brecciation.

Breccia fragments are cemented together by hematite, quartz, carbonate, chlorite, feldspar, mica, and other minerals. In most cases, clasts and wallrocks were hydrothermally altered, leading to metasomatic growth of secondary minerals including flecks of hematite or rhombs of dolomite. Widely disseminated earthy hematite and local potassic alteration in the breccia clasts resulted in color changes from original drab hues of gray and brown to striking pink and red. Clasts with embayments rimmed with secondary minerals such as specular hematite are evidence for the dissolution of clasts or their diagenetic cements by hydrothermal fluids. The main phase of

* Corresponding author. Tel.: +1-604-2915390; fax: +1-604-2914198.
E-mail address: dthorkel@sfu.ca (D.J. Thorkelson).

PII: S0301-9268(01)00155-3

brecciation and metasomatism occurred at ca. 1.6 Ga, as indicated by a 1595 ± 5 Ma U–Pb date on titanite. Subsequent minor hydrothermal events related to emplacement of the Hart River intrusions and Bear River dykes occurred at 1382.8 ± 7.4 Ma (U–Pb rutile) and ⩽ ca. 1270 Ma (U–Pb baddeleyite), respectively.

Mineralized breccias at and near the Olympic Dam deposit in South Australia mineralogically and texturally resemble, and have nearly the same age as, the Wernecke Breccias. These similarities suggest that both breccia provinces developed from related systems of hydrothermal activity, and provide additional evidence for models linking the cratons of North America and Australia in Proterozoic time.

Keywords: Proterozoic; Yukon; Rodinia; Breccia; Geochronology; Continental reconstructions

1. Introduction

Numerous breccia zones crosscut the Paleoproterozoic Wernecke Supergroup in northern Yukon (Fig. 1). They have previously been cited as key members of the Proterozoic iron oxide (Cu–U–Au–REE) deposit group by Hitzman et al. (1992). In the Wernecke Mountains, where our recent investigations have been concentrated, the breccia zones are collectively termed Wernecke Breccia. In the Ogilvie Mountains, 300 km to the west, similar breccias were termed the Ogilvie Mountains breccias by Lane (1990) but are herein regarded as a subset of Wernecke Breccia (Figs. 1 and 2). Individual breccia zones range in area from 0.1 to 10 km^2 and crop out in curvilinear arrays over an area of about 48 000 km^2 (Archer and Schmidt, 1978; Delaney, 1981; Bell, 1986a,b; Lane, 1990; Wheeler and McFeely, 1991; Thorkelson, 2000). Typical Wernecke Breccia consists of metasomatized, angular to subangular clasts in a hydrothermally precipitated matrix. Disseminated to fracture-controlled specular hematite is ubiquitous. The brecciation and related hydrothermal activity occurred in early Mesoproterozoic time, as detailed in this report.

This article is based on the results of a 1:50 000-scale geologic mapping program in the Wernecke Mountains (Figs. 1 and 2) between 1992 and 1996, and analytical work carried out during and subsequent to the mapping (e.g., Thorkelson and Wallace, 1993, 1995, 1998a,b,c; Abbott et al., 1997; Thorkelson et al., 1998; Thorkelson, 2000). Mineral occurrences referred to in this paper (shown in Fig. 2) are listed in Yukon Minfile (INAC, 1998). Mineralization in and around the breccia zones with variable enrichments in Cu, Co, U, and Au has been an intermittent focus of mineral exploration for many years. Similarities between Wernecke Breccia and other breccias of similar age and environment elsewhere in the world were noted by Bell and Jefferson (1987), Bell (1989), Gandhi and Bell (1990) and Hitzman et al. (1992). These authors drew connections between Wernecke Breccia and mineralized breccias at the giant Olympic deposit in Australia, on the basis of similar age, physical characteristics, mineralogy, and possible proximity between northwestern North America and Australia in Proterozoic time.

This paper reports new field, geochronological and petrological information on Wernecke Breccia that provides additional evidence for the proposed correlations between Mesoproterozoic assemblages in portions of northern Yukon and those in the Gawler Craton in South Australia. In particular, the new data provide support for reconstructions which place Australia next to northwestern Canada during the Proterozoic (e.g., Eisbacher, 1985; Bell and Jefferson, 1987; Moores, 1991; Young, 1992; Rainbird et al., 1996).

2. Geologic framework

2.1. Sedimentation, metamorphism and magmatism

Zones of Wernecke Breccia were emplaced into an upper crustal assemblage dominated by thick sedimentary successions of the Wernecke Supergroup (Fig. 3). The Wernecke Supergroup consists of three sedimentary groups with a cumulative thickness of about 13 km (Delaney, 1981; Norris and Dyke, 1997; Thorkelson, 2000). Mudstone, siltstone, and dolostone predominate, and form two clastic-to-carbonate grand cycles. The first grand cycle is evident in the ca. 4.8 km-thick Fairchild Lake Group, which began with mainly siltstone and progressed to brown- and white-weathering carbonate. The second grand cycle began with dark mudstone and siltstone of the ca. 3.4 km-thick Quartet Group, and ended with deposition of ca. 4.7 km of orange-weathering shallow-water carbonate of the Gillespie Lake Group (Delaney, 1981; Thorkelson, 2000). Overall, the Wernecke Supergroup appears to represent a gradual progression from rift basin to stable platform. Paleocurrent data suggest a principal source region to the north (Delaney, 1981).

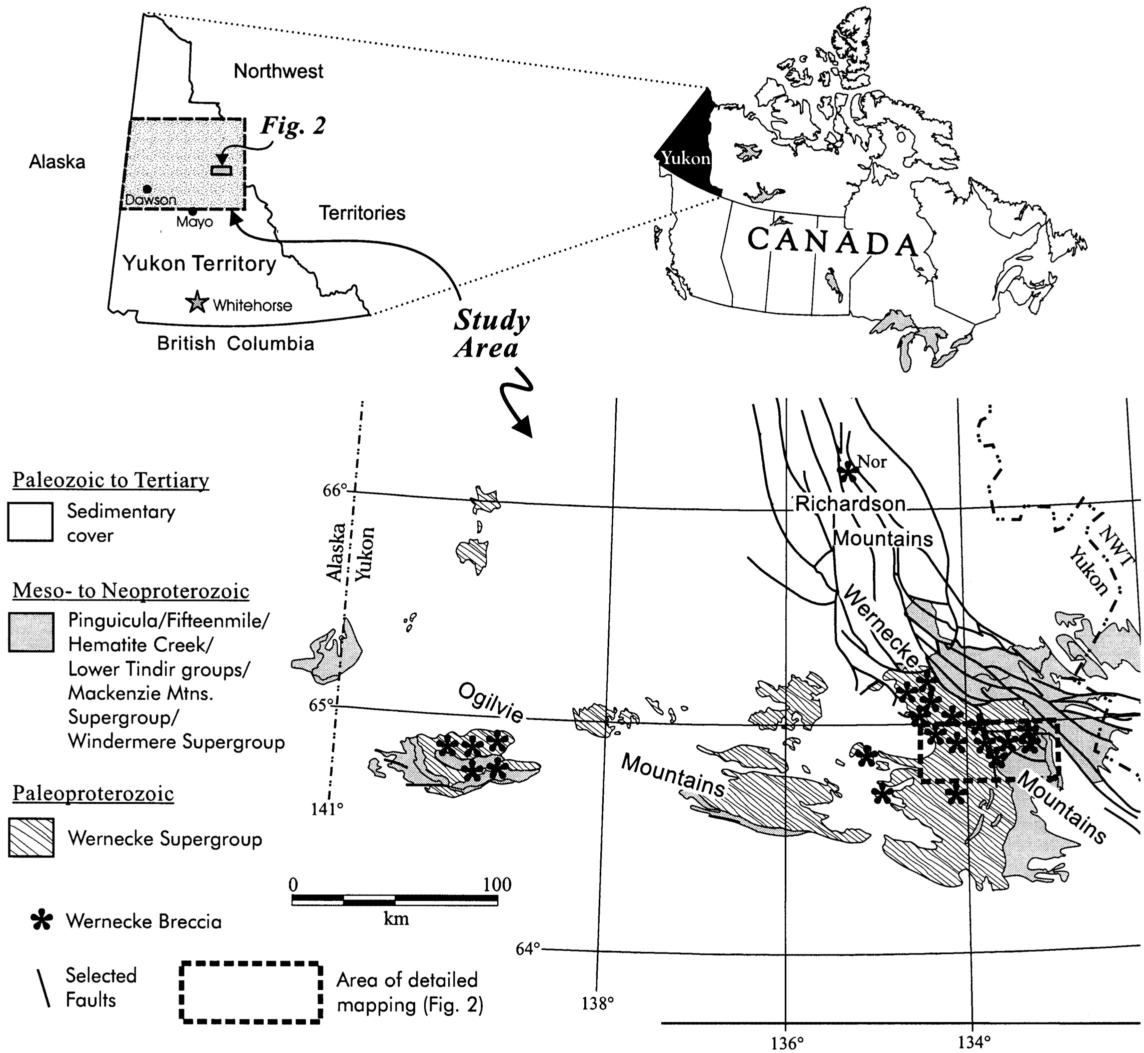

Fig. 1. Generalized geologic map of the study area in northern Yukon emphasizing Proterozoic inliers. Zones of Wernecke Breccia are hosted by Paleoproterozoic strata of the Wernecke Supergroup, and are schematically represented by asterisks. The Nor breccia occurrence is located in the Richardson Mountains. Area of recent investigations of Wernecke Breccia (Fig. 2) indicated by inset map.

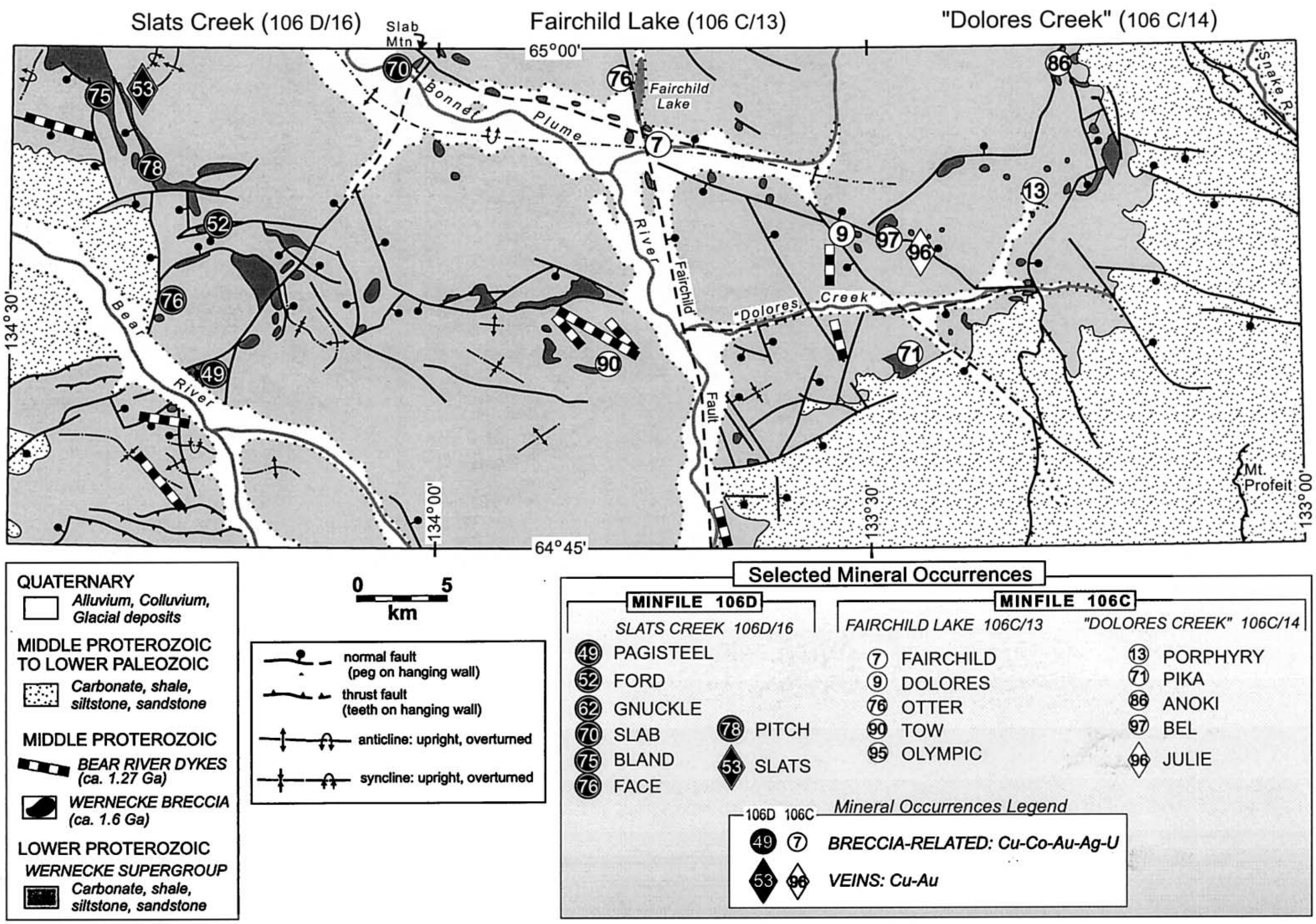

Fig. 2. Simplified geology of the northeastern Wernecke Mountains, showing locations of prominent Wernecke Breccia zones and selected mineral occurrences. Strata are grouped into pre- and post-Wernecke Breccia successions. The pre-breccia strata consist of the Lower Proterozoic Wernecke supergroup (and a small, downdropped block of the Slab volcanics, not shown, at Slab Mountain). The post-breccia strata comprise the Pinguicula, Hematite Creek, Windermere, Vampire and Franklin Mountain, and Mount Kindle successions, of Middle Proterozoic to Lower Paleozoic ages. Igneous intrusions of the Paleoproterozoic Bonnet Plume River suite occur within the Wernecke Supergroup and are commonly engulfed by Wernecke Breccia. Names and numbers of mineral occurrences are those provided in Yukon Minfile (INAC, 1998). All mineral occurrences mentioned in text are located on diagram except for the Gremlin and Igor occurrences which lie a few kilometers to the northwest.

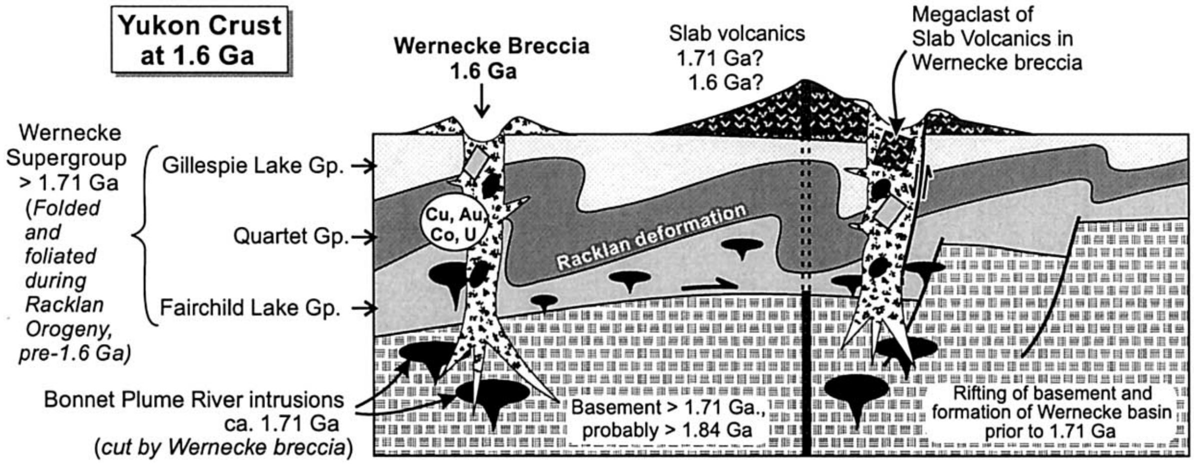

Fig. 3. Cartoon showing the main geologic features at the time of Wernecke Breccia emplacement, ≈1.6 Ga. Crystalline basement rifted to form the Wernecke basin and was infilled by the Wernecke Supergroup prior to ca. 1.71 Ga, when the earliest Bonnet Plume River intrusions were emplaced. The Slab volcanics may have been comagmatic with the Bonnet Plume River intrusions, or may be as young as 1.6 Ga. Racklan Orogeny produced southwest-directed folds, and local schistosity and kink-banding, in the Wernecke Supergroup prior to Wernecke brecciation. The timing of Bonnet Plume River magmatism relative to Racklan deformation is uncertain. The Wernecke Breccias crosscut the igneous rocks and the structures produced during Racklan Orogeny. Note the foundered megaclast of the Slab volcanics in one of the breccia zones. Metasomatic enrichments of Cu and other metals are localized. Surface features are nowhere preserved, and the presence of maar-like vents above the breccia zones is conjectural. Faulting may have been active during breccia emplacement and hydrothermal activity.

Prior to emplacement of Wernecke Breccia, the Wernecke Supergroup was intruded by the dioritic to syenitic Bonnet Plume River intrusions at ca. 1.71 Ga (Thorkelson, 2000), and overlain by the mafic- to intermediate-composition Slab volcanics (Fig. 3). The Slab volcanics and the Bonnet Plume River intrusions may be co-magmatic, as suggested by preliminary geochemical studies (Thorkelson, 2000). Alternatively, the Slab volcanics may be as young as ca. 1.6 Ga, the age of Wernecke Breccia. Before Wernecke brecciation, the region was deformed in the Racklan Orogeny (Gabrielse, 1967; Delaney, 1981; Cook, 1992; Norris and Dyke, 1997) prior to 1.6 Ga (Thorkelson et al., 1998; Thorkelson, 2000), a relation discussed further in this paper. Racklan deformation produced southeast-verging folds, localized schistosity, and kink-bands in the Wernecke Supergroup (Fig. 3; Gabrielse, 1967; Thorkelson, 2000). In regions of high strain, the Fairchild Lake Group was metamorphosed to fine-grained muscovite–chlorite–quartz schist with porphyroblasts of either garnet or chloritoid (Delaney, 1981). The timing of the Racklan Orogeny relative to the Bonnet Plume River and Slab igneous event(s) remains uncertain. Following Wernecke brecciation, the region was affected by episodes of Mesoproterozoic and Neoproterozoic magmatism, intervals of Mesoproterozoic and Paleozoic sedimentary deposition, and pulses of Proterozoic and Phanerozoic deformation, including Mesozoic to Early Cenozoic Cordilleran orogenesis. However, the area remained inboard of convergent plate-margin processes such as arc magmatism and terrane obduction.

2.2. Basement age and affinity

Crystalline basement beneath the sedimentary successions is nowhere exposed. Its age may range from Early Proterozoic to Archean. The great thickness and apparent continental affinity of the Wernecke Supergroup suggests that it was deposited in a marine basin (the Wernecke basin of Dredge Mitchelmore and Cook, 1994) that was underlain by attenuated continental crust, most probably a thinned, westward continuation of the North American craton (Fig. 3; Dredge Mitchelmore and Cook, 1994). Prior to the attenuation, the last major tectonic event to affect this part of the North American craton probably occurred during convergence and suturing of Precambrian terranes along the Fort Simpson, Wopmay and Trans-Hudson orogenic belts between 1.84 and 2.0 Ga (Hoffman, 1989; Villeneuve et al., 1991). Consequently, at about 1.84 Ga, the North American craton is likely to have extended westward beyond its current Cordilleran limit, and may have been sutured to the craton of another continent. Seismic reflection profiles to the east, extending from the Fort Simpson magmatic arc to the Slave craton, suggest that the Proterozoic sequences were deposited on a westward continuation of the ca. 1.84 Ga Fort Simpson magmatic terrane (Cook et al., 1998). Following deposition, lithospheric extension and crustal attenuation in the Yukon and adjacent areas probably signify initial separation of cratonic North America from continental crust to the west. The rifting produced deep intracratonic to possibly passive margin depocenters (Paleoproterozoic Wernecke basin; Paleo- to Meso-Proterozoic Muskwa basin (Bell, 1968; Long et al., 1999), and the Mesoproterozoic Belt–Purcell basin (Aitken and McMechan, 1992; Ross et al., 1992). Subsequent periods of extension during the Neoproterozoic to Early Paleozoic led to complete continental separation and development of a passive margin (Eisbacher, 1985; Ross, 1991).

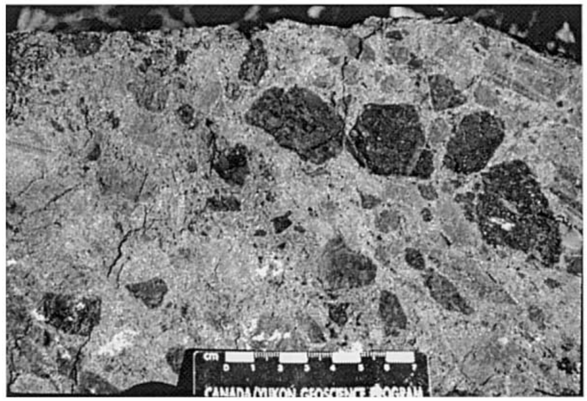

Fig. 4. Typical Wernecke Breccia from the Pika occurrence containing variably metasomatized clasts of siltstone and dolostone.

3. Wernecke Breccia

3.1. Physical and mineralogical characteristics

3.1.1. Breccia clasts

Breccia clasts are mainly derived from dolostone, siltstone, shale, slate, phyllite, and schist of the Wernecke Supergroup (Fig. 4). In addition, clasts of igneous intrusions are abundant locally (Fig. 5) where breccia zones crosscut or engulf dikes and stocks of the Bonnet Plume River intrusions (ca. 1.71 Ga). Volcanic clasts, derived from the Slab volcanics (possibly ca. 1.71 Ga), have been observed in one location (Fig. 3). In some localities, breccia clasts include those composed of previously cemented breccia. Clasts which could have been derived from underlying crystalline basement lithologies, such as gneiss or peridotite, are conspicuously absent.

Breccia clasts, at all localities, are set in a matrix composed of smaller rock fragments and a variety of hydrothermally deposited minerals which locally include chalcopyrite, cobaltite, and other minerals of economic interest. Clast colors vary from their source-rock colors of black, gray, brown, and green, to alteration-produced hues of

Fig. 5. intrusions in Wernecke Breccia (dark gray matrix) near the Olympic mineral occurrence. Field of view is ≈30 cm wide.

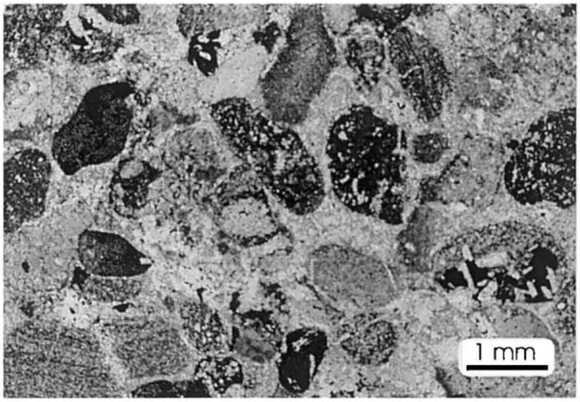

Fig. 6. Photomicrograph of well-rounded grains of variably metasomatized siltstone of the Wernecke Supergroup. Darkest grains contain greatest abundance of hematite. Plane-polarized light.

pink, red, and maroon, reflecting variable degrees of metasomatism. In most breccia zones, red and pink clasts are abundant, and secondary minerals such as dolomite and specular hematite are common as disseminations, fracture fillings, and veins. In many of the clasts, sedimentary laminations have been visually enhanced by preferential reddening of the coarser, more permeable layers. The red coloration is attributed to growth of disseminated earthy hematite and, in some cases, potassium feldspar. Wernecke Breccia is typically well-cemented and indurated. At the Slab, Otter and Fairchild occurrences, breccia is moderately friable and the clasts are typically drab gray – apparently containing little earthy hematite. These differences may reflect variations in temperature, pressure and composition of the hydrothermal fluids.

Clasts of country rock are typically angular to subangular, but are locally subrounded to rounded (Fig. 6). Clast rounding is attributed to abrasion with wallrock and "milling" among clasts during breccia activity. At several localities, clasts have marked embayments, and are commonly rimmed with specularite. The irregular shapes of these clasts, which contrast with the angular to rounded shapes of most other fragments, is consistent with soft-sediment deformation (Laznicka and Edwards, 1979). However, the Wernecke Supergroup, from which these clasts were derived, was fully lithified and locally metamorphosed prior to brecciation (details given below), hence the irregular, embayed clasts are better interpreted as products of aqueous corrosion or "digestion" during breccia-related hydrothermal activity (Laznicka and Edwards, 1979).

Clast sizes are generally in the granule, pebble and cobble size-ranges, although boulder-sized clasts are scattered in many breccia zones. Megaclasts (>2 m in diameter) of sedimentary or metamorphic rock are present in some of the breccia zones, notably at the Face and Slab mineral occurrences (Fig. 2). At the Slab mineral occurrence, megaclasts of schist and altered siltstone are common, some of which are 20 m or more across (Bell and Delaney, 1977). Megaclasts of intrusive rock are present in many of the breccia zones, including those at the Slab, Bel, Pika, Anoki, and Olympic mineral occurrences where blocks of Bonnet Plume River diorite up to 0.5 km long are engulfed by breccia. At the Slab occurrence, breccia surrounds a rotated megablock (0.25×0.6 km) of the Slab volcanics (Fig. 7).

3.1.2. *Metasomatic effects*

Large metasomatic aureoles are typically present in breccia zones and in surrounding country rock. Regionally, metasomatism began before and ended after brecciation, although specific metasomatic effects and timing differ among breccia zones. Generally, these effects include precipitation, in both clasts and matrix, of various phases including specular and earthy hematite, magnetite, dolomite, siderite, chlorite, biotite, muscovite, quartz, albite, microcline, rutile, titanite, brannerite, apatite, monazite, cobaltite, chalcopyrite, and (rare) bornite. Metasomatic porphyroblasts of specularite and dolomite are particularly common. Zones of massive specular hematite are present in some breccias, notably at the Pagisteel occurrence (Fig. 2). The igneous clasts in breccia zones are also typically metasomatized. Plagioclase is commonly replaced by albite, potassium feldspar or scapolite; augite is replaced by chlorite or actinolite; and carbonate, quartz, wollastonite, hematite and magnetite have developed preferentially as disseminations or along fractures.

Laznicka and Edwards (1979) examined breccias in and around the Dolores and Porphyry occurrences (Fig. 2) and concluded that metasomatism commonly led to sodium enrichment and potassium depletion. At the Porphyry site, albitized rock in the center of the aureole progressively gives way to rock enriched in quartz and sericite, and farther out, to rock enriched in quartz and carbonate. Crude zonation of alteration has also been documented at the Igor occurrence, a few kilometers northwest of the area in Fig. 2 (Hitzman et al., 1992; Laznicka and Edwards, 1979). Hitzman et al. (1992) developed a hydrothermal model based on sodic metasomatism (deepest), potassic metasomatism (middepth) and sericite–carbonate metasomatism (shallowest). However, their model is based partly on the premise that the Wernecke Supergroup was an undeformed 4.5-km thick layer-cake at the time of breccia formation, and that breccias present in the upper parts of the Wernecke Supergroup were emplaced at shallower levels of the crust. We now know that the Wernecke Supergroup ($\geqslant$13 km thick; Delaney, 1981; Thorkelson, 2000) was affected by at least two phases of contractional deformation of the Racklan Orogeny prior to brecciation (Thorkelson et al., 1998; Thorkelson, 2000). Folding and faulting during these events could have generated significant structural relief, bringing stratigraphically lower strata to the same level as, or higher than, stratigraphically higher rocks (similar to their present configuration).

Conly (1993) developed a generalized paragenetic sequence based on several specimens of breccia from the west side of the area in Fig. 2. Using optical and electron microscopy he determined that breccia matrix was dominated by early growth of feldspar, followed by quartz, mica, and carbonate, and late growth of mainly hematite. Chalcopyrite, in his depiction, grew in the middle and late stages of paragenesis. Additional studies are necessary to determine if these trends in zonation and paragenesis are common to other zones of Wernecke Breccia, and if mineralization can be correlated with depth.

Breccia matrix locally shows streaks defined by variations in grain size and mineral abundances, a feature probably generated by precipitation during fluid streaming. Late-stage quartz and carbonate veins commonly cut across both clasts and matrix of previously cemented breccias. Cu, Co, Au, Ag, and U minerals are locally enriched in the breccia and the associated metasomatic aureoles. Factors controlling metal distribution are

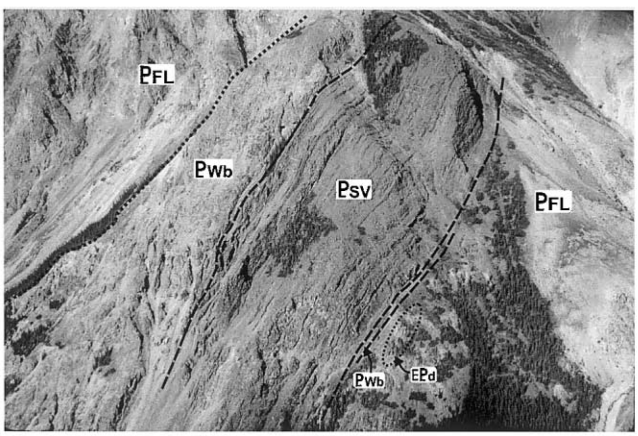

Fig. 7. Slab volcanics (PSV) of the SLAB mineral occurrence situated between Wernecke Breccia (PWb) and altered siltstone to kink-banded schist of the Fairchild Lake Group (PFL – lowest unit of the Wernecke Supergroup). A small body of the Bonnet Plume River intrusions (EPd) is located approximately. Thickness of Slab volcanics is about 250 m.

poorly understood, although gold concentrations generally correlate with those of copper (Appendix A-4 of Thorkelson, 2000).

3.1.3. Contacts and deformation

Contacts between breccia and country rock vary from abrupt to gradational. Some of the abrupt contacts are faults which juxtapose breccia with unaltered, unbrecciated strata, commonly of the Gillespie Lake Group. Others, however, are intrusive contacts between breccia and unaltered country rock. This relationship was noted near the Pitch and Slats occurrences (Fig. 2), where red-clast hematitic breccia intrudes unaltered siltstone and dolostone. Here, metasomatism of breccia clearly preceded and did not continue after breccia emplacement. The reverse relationship is recognized in the Slab occurrence, where relatively unaltered breccia was emplaced into metasomatized and mineralized (Cu, Co, U) rock. Crosscutting (intrusive) relations are evident at most locations, and are particularly well preserved at the Gremlin occurrence, 20 km northwest of the area of Fig. 2.

Gradational relationships between breccia and host rock are well developed in several places, especially around the Bland, Eaton, and Ford occurrences (Fig. 2). In such localities, unaltered host rock (typically dark siltstone) grades into altered host rock (typically purplish brown with red, bedding-controlled bands, and hematitic fractures), which grades into progressively more metasomatized and fractured rock toward the breccia. The transition from host rock to breccia is marked by a zone of crackle breccia in which highly fractured host rock has undergone incipient fragmentation. Metasomatic alteration increases toward the breccia zone, where clasts are typically reddened, and specular hematite is abundant, particularly in the matrix. The width of the metasomatic aureole from unaltered siltstone to Wernecke Breccia ranges from meters to hundreds of meters. In contrast, at the Gnuckle occurrence (Fig. 2), a zone of breccia is locally dominated by clasts of black shale that lack visible metasomatic effects. At this location, the shale clasts were apparently torn from country rock and rapidly cemented to form breccia without undergoing appreciable metasomatic alteration.

Petrofabrics indicate the timing of brecciation relative to other deformational events. Specifically, randomly oriented clasts of kinked schist and slate of the Fairchild Lake Group occur in Wernecke Breccia at the Slab and Julie occurrences. The matrix of the breccia at these locations is devoid of secondary petrofabrics, indicating that synkinematic metamorphism and kinking, from the first and second phases of deformation of the Racklan Orogeny, preceded brecciation (Fig. 3; Thorkelson, 2000).

3.1.4. Style of breccia emplacement

Previous workers have suggested various modes of occurrence for Wernecke Breccia, including diatremes (Bell and Delaney, 1977; Tempelman-Kluit, 1981), phreatomagmatic explosions (Laznicka and Edwards, 1979), modified evaporite diapirs (Bell, 1989), or mud diapirs (Lane, 1990). The hypothesis of mud diapirism is untenable because the Wernecke Supergroup was lithified and locally metamorphosed at the time of brecciation. The hypothesis of evaporate diapirism is rejected because brecciation occurred after formation of cleavage, schistosity, kink bands, upright to overturned folds, and lower greenschist-grade metamorphism of the Racklan Orogeny – processes which would have destroyed the chemical character and physical continuity of the hypothetical salt beds.

Phreatomagmatic explosion as the cause of brecciation is appealing because it recognizes the close spatial relationship between the Bonnet Plume River intrusions (mainly diorite) and Wernecke Breccia. The igneous intrusions typically occur as mega-clasts in breccia, or as small dikes and stocks near breccia zones. This spatial coincidence led Laznicka and Edwards (1979) and Laznicka and Gaboury (1988) to suggest that magmas that were emplaced into unconsolidated sediment of the Wernecke Supergroup triggered phreatomagmatic explosions and formation of Wernecke Breccia. Although this explanation accounts for the spatial relationship between the breccias and the igneous intrusions, it is rejected for three reasons. Firstly, the intrusions were emplaced about 100 Ma prior to the oldest isotopic age of hydrothermal activity, and presumably breccia formation. Secondly, the

Wernecke Supergroup was entirely lithified, twice deformed, and variably metamorphosed to lower greenschist grade before brecciation. Thirdly, no chilled igneous clasts or hyaloclastite have been observed, despite considerable petrographic investigation.

The rejection of the unconsolidated/phreatomagmatic model leaves unresolved the issue of the spatial juxtaposition of the breccias and the igneous intrusions. Perhaps the best explanation is that the hydrothermal solutions responsible for brecciation rose through the crust along the same pathways used previously by the magmas. Deep-seated fracture systems may have developed prior to or during igneous activity, and may have acted as long-lived "plumbing systems" for subsequent metasomatic events.

The diatreme model of breccia genesis (Bell and Delaney, 1977; Tempelman-Kluit, 1981) is consistent with much, but not all, of the existing data. A diatreme origin can account for the following: (1) intrusion of breccia into a succession of rock which had previously undergone deformation and igneous intrusion; (2) intense fracturing of country rock; and (3) rounding of clasts by milling within moving breccia. However, two principal features of the breccias require qualification of this model. Firstly, breccia clasts were derived from the Wernecke Supergroup and the igneous intrusions it hosts. Importantly, clasts of lower crustal or mantle affinity, such as gneiss or peridotite, have not been reported from any of the breccias. Consequently, the clastic component of Wernecke Breccia appears to have originated almost entirely within Wernecke Supergroup, although a deeper source for the mineralizing fluids is plausible. Secondly, the breccia zones are distributed in curvilinear arrays that are typically related to steep faults (Delaney, 1981; Lane, 1990). This style of distribution implies a strong supracrustal influence on the location of breccia development. Furthermore, breccia zones do not decrease in size and abundance with increasing depth. Zones of Wernecke Breccia thereby differ from typical diatremes which are generally depicted as downward-tapering conical pipes (Mitchell, 1991).

Wernecke Breccia is most favorably modeled as a set of hydrothermal-phreatic breccias whose location was partly determined by crustal features. Brecciation was probably caused by explosive expansion of volatile-rich fluids. Venting of the breccia may have occurred above the Slab volcanics or correlative strata. A mafic igneous influence is implied by common enrichments in Fe, Cu and Co. The fluids may have been partly derived from volatile-rich residual liquids of fractionating tholeiitic magma chambers located beneath the Wernecke Supergroup (cf. Hitzman et al., 1992; Thorkelson and Wallace, 1993). Breccia generation could represent a late magmatic stage, when the chambers were largely solidified, and fluids enriched in Fe and volatiles escaped toward the surface and boiled explosively.

Some previous authors described individual breccia zones according to textures and apparent genetic affinity, using descriptors such as crackle breccia, mosaic breccia, slurry breccia, channel-way breccia, pebble dikes, stope breccia and fault breccia (e.g., Delaney, 1981; Laznicka and Gaboury, 1988; Lane, 1990). Any of these terms may be applicable to specific breccia zones, but, as noted by Laznicka and Gaboury (1988), all of the breccia types are best considered within a spectrum from "fractured protolith" to "transported breccia," and all are favorably accommodated within a regime of explosive hydrothermal activity.

Many of the important geologic relationships surrounding Wernecke Breccia are illustrated in Fig. 8, a generalized cross-section through the Pika mineral occurrence. At the Pika, breccia crosscuts previously deformed dolostone of the Gillespie Lake Group (Wernecke Supergroup), and dioritic intrusions of the Bonnet Plume River suite. Small areas of hypogene copper enrichments in the form of chalcopyrite are scattered about the breccia, and are commonly in greatest abundance along the margins of the diorite. A weak supergene oxide layer characterized by malachite coatings is present a few meters beneath the unconformity with the overlying Mesoproterozoic Pinguicula Group. Subsequent open folding has affected the entire section.

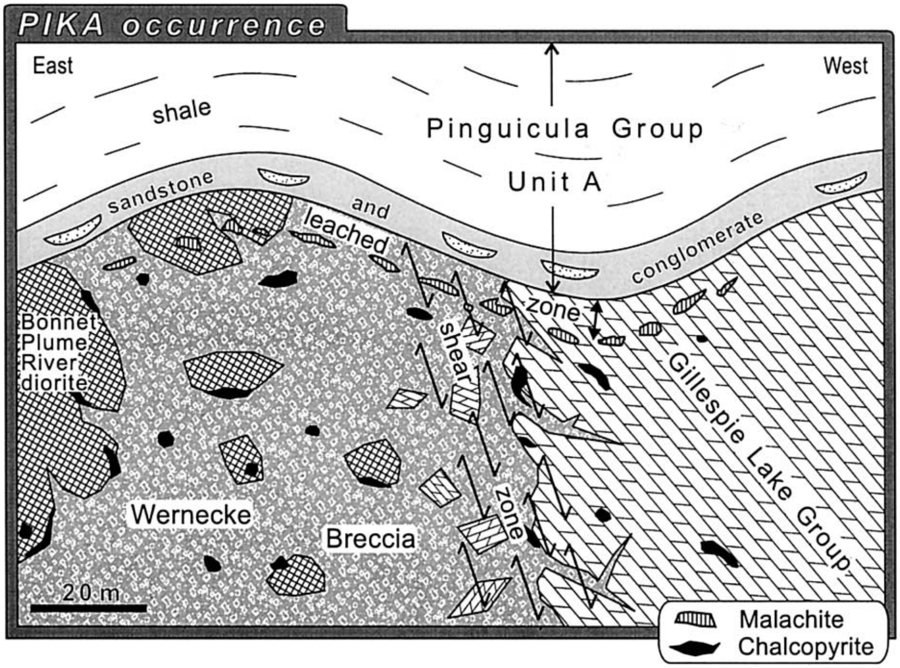

Fig. 8. Geologic relations at the Pika mineral occurrence. The geologic history of this area includes: (1) deposition of the Gillespie Lake Group (Wernecke Supergroup); (2) intrusion of Bonnet Plume River diorite, and deformation during Racklan Orogeny (order uncertain); (3) emplacement of Wernecke Breccia, metasomatism of breccia and host rock, and hydrothermal precipitation of chalcopyrite; (4) localized shearing; (5) deep weathering, and leaching of copper from chalcopyrite to form a weak supergene-oxide zone of malachite; (6) deposition of the Pinguicula Group; and (7) regional folding.

3.2. Timing of brecciation and hydrothermal activity

3.2.1. Introduction

Field observations and isotopic dates from this investigation have added important constraints to the timing of geological events related to breccia genesis. Previously, the only reliable isotopic date was a U–Pb monazite age of 1270 ± 40 Ma from the Nor breccia in the Richardson Mountains (Fig. 1; Parrish and Bell, 1987). Although the date is considered analytically sound, its relevance to the breccia province as a whole was uncertain because the Nor breccia is about 130 km from the closest zones of Wernecke Breccia. Other isotopic dates on U-bearing whole rocks and minerals such as brannerite and pitchblende were reported by Archer et al. (1986). Their oldest date approached 1200 Ma, but most were much younger. The highly discordant nature of these dates renders them difficult to interpret, and they are considered unreliable estimates of the ages of initial brecciation and subsequent hydrothermal activity (Parrish and Bell, 1987).

Three isotopic dates reveal that hydrothermal activity in Wernecke Breccia zones occurred in at least three pulses. Titanite (sphene) from the breccia zone on the eastern side of the Slab mineral occurrence (Fig. 7) was dated at ca. 1595 Ma. This date is interpreted as the time of initial brecciation and hydrothermal activity, although earlier events cannot be precluded. The second date was from the Slab volcanics, which lie as a megaclast within the breccia at the Slab occurrence. Rutile from intermediate-composition lava was dated at ca. 1383 Ma, and is considered to represent a second pulse of hydrothermal activity within the Slab breccia zone. The third date is from a Bear River dike in the northwestern part of the study area, 2 km south of the Bland mineral occurrence. Baddeleyite from the dike was dated at ca. 1270 Ma (Thorkelson, 2000). The dike, which lies about 1 km from a breccia zone, is crosscut by veinlets of earthy and specular hematite, features which characterize much of the hydrothermal activity associated with Wernecke Breccia bodies. The baddeleyite date is considered to be the time of dike solidification, and therefore constrains the age of this metasomatism to be ca. 1270 Ma or later.

3.2.2. Metasomatism at 1.6 Ga in the Slab Mountain breccia

Titanite is abundant in the hydrothermally precipitated matrix of Wernecke Breccia at Slab Mountain. Some grains are euhedral (Fig. 9) whereas others are anhedral and appear to have grown interstitially among grains of quartz, feldspar and biotite. A titanite concentrate was obtained from a ~20 kg sample of breccia (DT93-7-16c). The titanite grains vary in color from nearly colorless to dark orange–brown. Confirmation of mineral identity was made for both colorless and colored types by X-ray diffraction. Fractions were picked from this concentrate to sample the range in color variation, and five U–Pb isotopic analyses were made at the University of Alberta. U–Pb laboratory methodology is provided in Yamashita et al. (2000).

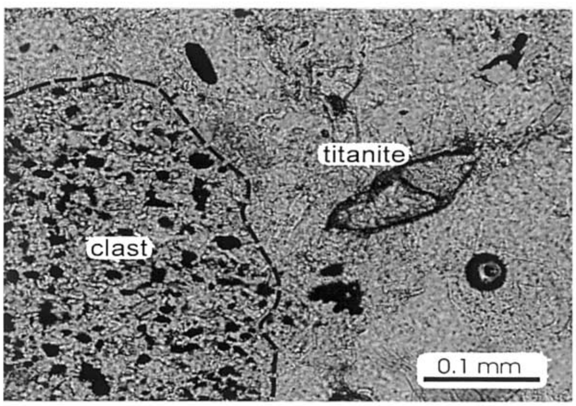

Fig. 9. Photomicrograph of euhedral titanite grain in hydrothermally precipitated matrix of Wernecke Breccia at Slab Mountain. Matrix is dominated by microcline, albite, biotite, quartz, and hematite. Clast of siltstone, probably from the Wernecke Supergroup, contains abundant metasomatic hematite (opaque) and biotite. Plane-polarized light.

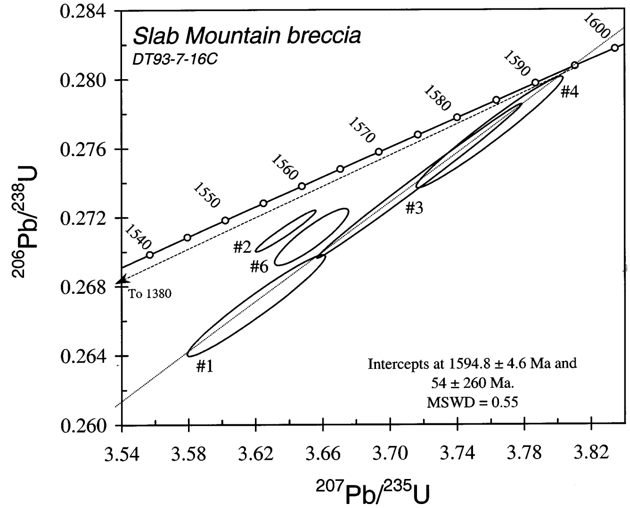

Fig. 10. U–Pb concordia showing analyses derived from five fractions of hydrothermal titanite separated from breccia sample DT93-7-16C. A regression line through fractions #1, #3 and #4 yields a concordia upper intercept age of 1594.8 ± 4.6 Ma, with an MSWD of 0.55 (dotted line). Also shown is a Pb-loss trajectory between 1595 Ma and ~1380 Ma (dashed line); refer text for details.

The five titanite fractions have U contents of 46–217 ppm, with the nearly colorless fraction having the lowest U content (Table 1). The amount of total common Pb is low to moderate, at 57–185 pg, and the $^{206}Pb/^{204}Pb$ ratios range from ~2400 to 11 000 (Table 1); the five analyzes are shown on a concordia diagram in Fig. 10. It is apparent from Fig. 10 that three analyzes define a linear array (analyzes 1, 3 and 4) with an upper concordia intercept of ~1595 Ma. The individual $^{207}Pb/^{206}Pb$ model ages for these three samples are 1594, 1594 and 1596 Ma, respectively, and they range from 4.9% discordant to 1.4% discordant (Table 1). The least discordant analysis of the three is fraction #4, which was abraded prior to analysis. Regression of these data yield a line with an upper concordia intercept age of 1594.8 ± 4.6 Ma using the program ISOPLOT (Ludwig, 1998). These three analyzes are very well fitted to the regression line, as indicated by the low MSWD value of 0.55. The remaining two fractions (#2, #6) plot above the 1595 Ma regression line with younger $^{207}Pb/^{206}Pb$ model ages of 1573 and 1583 Ma, respectively, but with similar degrees of discordance (2–3%; Table 1).

Table 1
Titanite U–Pb isotopic data from Slab Mountain breccia sample DT93-7-16C[a]

Fraction	Description	Grains	Weight (mg)	U (ppm)	Pb Rad. (ppm)	Pb[a] Com (pg)	Th/U[b]	$^{206}Pb/^{204}Pb$[c]	$^{206}Pb/^{238}U$[d] ($\pm 1\sigma$)	$^{207}Pb/^{235}U$[d] ($\pm 1\sigma$)	Model age $^{206}Pb/^{238}U$	Model age $^{207}Pb/^{235}U$	Model age $^{207}Pb/^{206}Pb$	% Disc.
#1	Near-colorless, not abraded	20	0.467	46.0	14.89	150.7	1.02	2403	0.2669 ± 0.0012	3.6205 ± 0.0168	1525	1554	1594	4.9
#2	Dark, not abraded	18	0.300	216.9	67.78	101.3	0.80	10929	0.2712 ± 0.0005	3.6380 ± 0.0073	1547	1558	1573	1.9
#3	Dark, not abraded	60	1.02	93.12	30.59	165.0	0.97	9903	2741 ± 0.0018	3.7177 ± 0.0250	1561	1575	1594	2.3
#4	Dark, abraded	20	0.461	92.74	30.02	185.3	0.86	4018	0.2769 ± 0.0013	3.7596 ± 0.0179	1576	1584	1596	1.4
#6	Dark, not abraded	20	0.331	98.7	31.23	57.11	0.86	9707	0.2708 ± 0.0007	3.6534 ± 0.0090	1545	1561	1583	2.7

Note: Decay constants are those recommended by Steiger and Jäger (1977).
[a] Total common Pb in sample (blank plus initial Pb).
[b] Model Th/U ratio based on observed abundance of ^{208}Pb.
[c] Corrected for spike and mass fractionation only.
[d] Corrected for spike, blank and mass fractionation.

These data indicate that some complexity exists in the U–Pb systematics of titanite from this sample that is not obviously related to a simple physical property such as color, as both near-colorless and more strongly colored fractions comprise the 1595 Ma regression. No physical evidence of multiple growth phases could be recognized, such as core–rim relationships within grains of the concentrate. With the available data, we interpret the U–$Pb_{titanite}$ results to indicate formation of hydrothermal titanite at 1595 Ma, followed by either of two possibilities. Firstly, that the hydrothermal solutions capable of crystallizing titanite persisted to a time younger than 1595 Ma, resulting in the two titanite fractions with $^{207}Pb/^{206}Pb$ model ages of 1573 and 1583 Ma. If this is the case and titanite fractions are being selected from a concentrate with a range of true crystallization ages, then the likelihood of selecting three fractions, each comprising 20–60 grains, containing none of the <1595 Ma growth phases, seems remote. A second explanation is that titanite has suffered a complex Pb-loss history after hydrothermal crystallization at 1595 Ma. The three fractions with the well-defined age of 1595 Ma have a lower concordia intercept with error of modern Pb-loss (54 ± 260 Ma). The analyzes of fractions 2 and 6 could be explained if these samples suffered Pb-loss at a time younger than 1595 Ma, but prior to modern Pb-loss. As an example, a Pb-loss trajectory is shown between 1595 Ma and ~ 1380 Ma, the time of hydrothermal rutile growth in the Slab volcanics (see below). Fractions 2 and 6 fall between this putative 1380 Ma Pb-loss line and the 3-analysis 1595 Ma regression line. Without further detailed work, the true cause of the complex U–Pb systematics in hydrothermal titanite remains unresolved.

3.2.3. Metasomatism at 1.38 Ga of the Slab volcanics

A heavy mineral concentrate was prepared from a 25-kg sample of a weakly altered lava flow of the Slab volcanics. The sample was taken from the foundered volcanic megaclast in the Slab Mountain breccia. The concentrate yielded no zircon but did yield a small amount of rutile. The rutile grains are slender euhedral prisms up to 74 microns in length that range from pale to dark reddish brown in color. Five unabraded fractions of rutile were analyzed using U–Pb methods at the University of British Columbia (Mortensen et al., 1995). Procedural blanks were 8–4 pg for Pb and 1 pg for U.

Table 2
U–Pb analytical data from rutiles from Slab volcanics sample DT-93-25-1C

Fraction	$^{238}U/^{204}Pb$ ($\pm 1\sigma$)	$^{206}Pb/^{204}Pb$ ($\pm 1\sigma$)	Correlation coefficient
A	6408.3 (0.90)	1545.1 (0.80)	0.99
B	1304.8 (0.43)	327.2 (0.43)	0.95
C	1541.2 (0.78)	379.3 (0.75)	0.95
D	931.4 (0.61)	245.8 (0.61)	0.99
E	856.6 (0.63)	215.9 (0.63)	0.98

Five fractions of rutile contain moderate concentrations of U but highly variable amounts of initial common Pb, as evidenced by the $^{206}Pb/^{204}Pb$ ratios (Tables 2 and 3). The composition of this initial common Pb is unknown, but introduces considerable uncertainty into calculated U–Pb ages for each fraction. To better interpret the results and to avoid the necessity of fore-knowledge of the composition of the initial common Pb component in the rutiles (cf. Stacey and Kramer, 1975), U–Pb data are plotted on a $^{238}U/^{204}Pb$ vs. $^{206}Pb/^{204}Pb$ isochron plot in Fig. 11. Errors at-

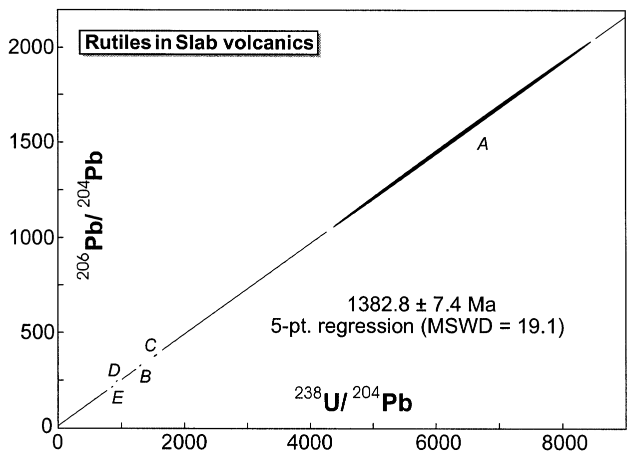

Fig. 11. U–Pb isochron plot for hydrothermal rutiles from a sample of Slab Volcanics.

Table 3
U–Pb analytical details of rutile grains from the Slab volcanics sample DT-93-25-1C[a]

Sample description[a]	Wt (mg)	U content (ppm)	Pb[b] content (ppm)	$^{206}Pb/^{204}Pb$ (meas.)[c]	Total common Pb (pg)	% ^{208}Pb[b]	$^{206}Pb/^{238}U$[d] ($\pm$% 1σ)	$^{207}Pb/^{235}U$[d] ($\pm$% 1σ)	$^{207}Pb/^{206}Pb$[d] ($\pm$% 1σ)	$^{206}Pb/^{238}U$ age (Ma; $\pm$% 2σ)	$^{207}Pb/^{206}Pb$ age (Ma; $\pm$% 2σ)
A: N2, +105	0.010	286	4.3	369	7	16.6	0.01403 (0.17)	0.09250 (1.06)	0.04781 (0.98)	89.8 (0.3)	89.8 (46.6)
B: N2, +105	0.007	267	4.0	397	4	15.0	0.01403 (0.25)	0.09250 (1.09)	0.04783 (1.02)	89.8 (0.4)	90.8 (47.9)
C: N2, 74–105, u	0.062	310	4.5	1795	9	13.3	0.01395 (0.12)	0.09198 (0.23)	0.04780 (0.15)	89.3 (0.2)	89.5 (7.1)
D: N2, 74–105, u	0.052	289	4.3	1592	8	15.1	0.01398 (0.10)	0.09154 (0.29)	0.04781 (0.24)	88.9 (0.2)	89.6 (11.2)

[a] N1, N2 = non-magnetic at given degrees side slope on Frantz isodynamic magnetic separator; grain size given in microns; u = unabraded.
[b] Radiogenic Pb; corrected for blank, initial common Pb, and spike.
[c] Corrected for spike and fractionation.
[d] Corrected for blank Pb and U, and common Pb.

tached to individual analyzes were calculated using the numerical error propogation method of Roddick (1987), and decay constants used are those recommended by Steiger and Jäger (1977). All errors are given at the 2σ level.

The five rutile fractions define a reasonably linear array on the isochron plot (Fig. 11). A calculated regression through the data gives a MSWD of 19.1, and a slope which corresponds to an age of 1382.8 ± 7.4 Ma. The calculated error for a standard York-II model regression has been expanded by multiplying by the square root of MSWD in order to account for the scatter in the data (Parrish et al., 1987). The age of ca. 1383 Ma is considered to be the crystallization age of rutile in the sample.

3.2.4. Synthesis of age determinations

Almost all of the brecciation and metasomatism occurred during the earliest event (ca. 1.6 Ga). This relationship is evident from the nature of the contact between Wernecke Breccia and the Pinguicula/lower Fifteenmile groups. The contact is well exposed at several places in both the Wernecke and Ogilvie mountains. The basal Pinguicula and Fifteenmile strata (ca. 1.38 Ga; Thorkelson, 2000) nonconformably overlie the breccia, and there is no evidence that hydrothermal activity at those localities continued after Pinguicula/Fifteemile deposition (Thorkelson, 2000). Furthermore, a well-developed regolith and weathered zone is locally present at the top of the breccia zones, confirming that the main cycle of brecciation and hydrothermal activity ended prior to Pinguicula/Fifteenmile sedimentation (Thorkelson and Wallace, 1993). The subsequent hydrothermal events at ca. 1.38 Ga and ≤ 1.27 Ga are nowhere observed to crosscut the Pinguicula or Fifteenmile strata (these units do not crop out near the sites of the younger alteration). The 1.27 and 1.38 Ga hydrothermal events are therefore considered to be minor and very localized.

The surges of hydrothermal fluids that brecciated and mineralized the Wernecke Supergroup were produced in a huge area of crust, spanning the Wernecke, Ogilvie and part of the Richardson mountains. The fluid surges were probably generated by a sudden event of crustal heating. The simplest explanation for rapid heating is regional upwelling of mantle and emplacement of mafic igneous intrusions in the lower crust. A magmatic episode at the time of breccia formation (ca. 1.6 Ga) is not recognized in Yukon, although the undated Slab volcanics (Figs. 3 and 7), with a permissive age-range of 1.6–1.71 Ga, are the only igneous rocks known in the region which could represent breccia-age magmatism. A hint of magmatic activity at ca. 1.6 Ga is inferred from the inheritance age of zircons in a granitic clast, with a crystallization age of ca. 1.15 Ga, from the Coates Lake diatreme of probabe Paleozoic age, located ≈ 350 km southeast of the Wernecke Mountains in the Mackenzie Mountains of the Northwest Territories (Jefferson and Parrish, 1989). Conceivably, intrusive igneous rocks that may have triggered the hydrothermal activity and brecciation are restricted to the middle and lower crust, and remain unexposed, as proposed by Laznicka and Gaboury (1988).

The hydrothermal events following 1.6 Ga brecciation may be tied to more local igneous events. Metasomatism at 1380 Ma was probably associated with emplacement of the 1380 Ma Hart River mafic intrusions (Abbott, 1997) which crop out 25–50 km to the south and southwest of Fig. 2 (Green, 1972). Subsequent metasomatism, at ca. 1270 Ma in the Richardson Mountains, and at ca. 1270 Ma or later in the study area, is most favorably linked to emplacement of the Bear River dikes which intruded the western and central parts of the area in Fig. 2 at ca. 1270 Ma. These dikes may be part of the large 1267 ± 2 Ma Mackenzie igneous event which includes the Muskox intrusion, the Coppermine lavas, and the giant radiating Mackenzie dike swarm of the Northwest Territories and adjacent parts of the Canadian Shield (LeCheminant and Heaman, 1989; Francis, 1994). Approximately 15 Bear River dikes have been identified. They are typically 2–6 km long, several meters wide, and strike mainly to the northwest. The 1380 and 1270 Ma events reflect episodic flow of hydrothermal solutions along igneous pathways and through the breccia zones.

3.3. Model for brecciation and mineralization

A model relating igneous events, brecciation, and mineralization is presented here. In the first stage (pre-breccia stage), mineralization related to intrusive events preceded Wernecke brecciation. In this stage, dioritic intrusions were emplaced at ca. 1.71 Ga, and the Slab volcanics erupted between ca. 1.71 and 1.6 Ga. During this interval, probably during one or both of these igneous events, Cu–Co–Au mineralization occurred as fracture fillings and disseminations in the Wernecke Supergroup in a manner similar to Cu–porphyry systems. Pre-breccia mineralization is well displayed at the Slab occurrence (Fig. 2), where the Wernecke Supergroup and Bonnet Plume River diorite are mineralized, but the main crosscutting body of Wernecke Breccia is not. Pre-breccia metasomatic activity may have been localized rather than widespread.

In the second stage (main brecciation), a large pulse of rising Fe-rich fluids expanded explosively at ca. 1.6 Ga (Fig. 3). These volatile explosions produced numerous subterranean breccia zones whose initial porosity ranged from 10 to 70%. Widespread metasomatism and hydrothermal precipitation preceded, accompanied, and followed the brecciation. In some zones, brecciation occurred several times, as indicated by breccia clasts composed of previously cemented breccia. Faults were probably active concurrently, and may have served to focus hydrothermal flow and breccia formation (Delaney, 1981; Lane, 1990; Hitzman et al., 1992). Following Hitzman et al. (1992), we speculate that the faults may have breached, perhaps episodically, hydrothermal lenses or aquifers, permitting supercritical fluids to rise and expand explosively, brecciating the country rock. Fractionation of water from igneous intrusions and the dehydration of hydrous minerals during prograde metamorphism at depth may have generated excess fluid pressures in the upper crust. Whereas the rising of hot, overpressured fluids may have been largely triggered by faulting, the widespread abundance of hydrothermal fluids is likely to be the result of a regional thermal event involving igneous intrusions (Hitzman et al., 1992), possibly related to regional upwelling of asthenospheric mantle.

Venting above the breccia zones almost certainly occurred, perhaps forming maar-like explosion pits above the Slab volcanics or the Wernecke Supergroup. (Vent deposits are nowhere preserved because of extensive Middle and Late Proterozoic denudation.) Mineralization of Cu, Co, Au or U occurred during the hydrothermal activity. Most or all of the breccia zones are considered to have developed during this stage, as younger rocks are generally unaffected by brecciation and metasomatism.

In the third and fourth stages (late hydrothermal flow), the breccia zones served as conduits for localized hydrothermal fluids generated during the 1.38 Ga (Hart River) and 1.27 Ga (Bear River-Mackenzie) igneous events (Abbott, 1997; Parrish and Bell, 1987). Geisers, hotsprings, and volcanoes may have been active concurrently, but no record of these possible surficial features remains. Additional Cu, Co, Au or U mineralization may have occurred during these stages. However, concomitant brecciation has not been documented, and cannot have been widespread.

3.4. Mineral enrichments

Enrichments of Cu, Co, Au, Ag, Mo and U are localized within breccia zones and adjacent metasomatized country rock. The mineralizing events occurred chiefly in the main period of breccia formation and metasomatism. The absence of Fe–Cu–Co–Au–Ag–U enrichments in the Pinguicula Group, which was unconformably deposited on the breccia and its host rocks at ca. 1.38 Ga, is strong evidence that the vast majority of "breccia-related" mineralization occurred in the main stage of fluid flux, at ca. 1.6 Ga. Copper occurs as chalcopyrite, malachite, and rarely as bornite and chalcocite; cobalt occurs as cobaltite and erythrite; and uranium occurs as brannerite, uraninite, and related secondary minerals. Molybdenum occurs as molybdenite. Gold and silver concentrations are generally dependent on copper abundances (Thorkelson, 2000).

The metasomatic alteration which is so characteristic of the breccia zones did not produce significant increases in the background concentrations of

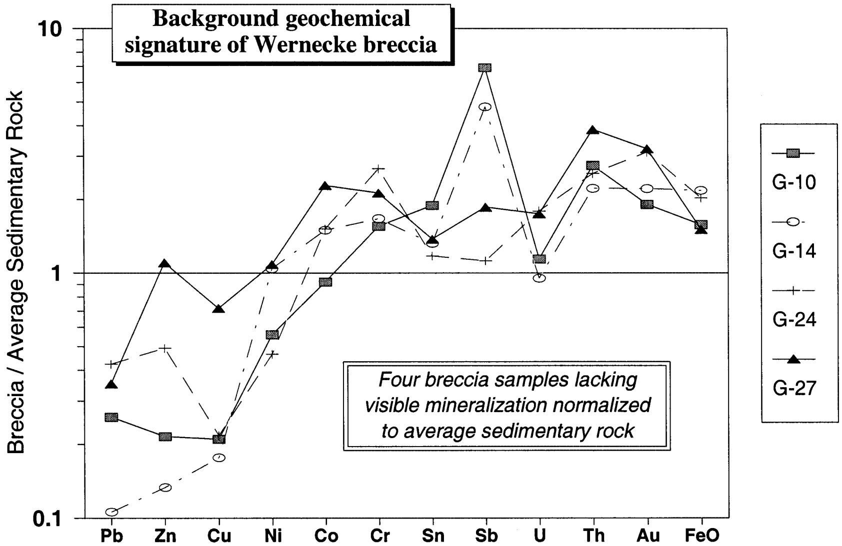

Fig. 12. Background metallic element concentrations in metasomatized but visibly non-mineralized samples of Wernecke Breccia. Concentrations in breccia samples are divided by those in worldwide-average sedimentary rock, taken from various sources. Normalizing values: 12 ppm Pb, 44 ppm Zn, 18 ppm Cu, 30 ppm Ni, 6.5 ppm Co, 45 ppm Cr, 2.3 ppm Sn, 0.58 ppm Sb, 2.1 ppm U, 5.1 ppm Th, 10 ppm Au, 4% FeO (total Fe as FeO).

metallic elements in the breccias. Low background levels in Wernecke Breccia were established by Thorkelson and Wallace (1993). In their study, concentrations of Pb, Zn, Cu, Ni, Co, Cr, Sn, Sb, U, Th, Au and FeO in four hematitic breccia samples from the western part of Fig. 2 were normalized to average sedimentary rock (Fig. 12). All of the samples contain sedimentary clasts that are highly reddened, probably from hematitic and possibly potassic alteration, but none were visibly enriched in base or precious metals other than Fe. None of the samples have concentrations of any element greater than ten times the sedimentary normalizing values. In contrast, the strongly mineralized parts of the breccias commonly contain enrichments of Cu, Co, U, or Au which are hundreds or thousands of times higher than normal "background" levels. These data indicate that breccia-related hydrothermal alteration did not ubiquitously raise the concentrations of metallic elements. Local variations in country rock or perturbations in hydrothermal activity are likely to have controlled the distribution of Fe, Cu, Co, U and Au mineralization. The timing and compositional characteristics of mineralization relative to the more widespread iron–alkali–carbonate–chorite–silica alteration has not been determined. Studies of mineral paragenesis suggest that the metal enrichments occurred late in the history of initial hydrothermal activity (Laznicka and Edwards, 1979; Conly, 1993; Conly et al., 1995).

The presence of igneous rock in and near the breccia zones has locally enhanced Cu mineralization. This relationship is established at the Porphyry, Olympic, Fairchild, Dolores and Pika occurrences (Figs. 2 and 8), where Cu showings commonly occur within or adjacent to bodies of fine- to medium-grained diorite and quartz albite syenite, fine-grained anorthosite, and fine-grained biotitic mafic dikes, mainly of the Bonnet Plume River intrusions. Apparently, the composition of these igneous bodies was particularly suitable for deposition of Cu from mineralizing fluids.

Some of the Cu in these occurrences may represent local redistribution of Cu within the intrusions (Laznicka and Edwards, 1979). However, some of the Cu was probably also derived from the hydrothermal fluids. This contention is supported by strong Cu enrichments in areas of breccia apparently distal from igneous rock. At the Tow occur rence, for example, no igneous rocks are exposed, yet chalcopyrite is abundant as disseminated grains within siliceous breccia matrix. The source of Cu in the hydrothermal fluids responsible for this mineralization is unknown. Possibly, Cu was leached from igneous intrusions at depth. The source of Cu and other elements in Wernecke Breccia may be principally of igneous origin or derivation. This possibility is supported by the common spatial association between breccia bodies and igneous intrusions (Laznicka and Gaboury, 1988; Lane, 1990), which suggests that many of the breccias developed in zones of crustal weakness previously intruded by stocks and dikes.

4. Australian connection?

Numerous breccia zones of hydrothermal origin are present in South Australia's Olympic Subdomain, an informal term referring to the mineralized region of the Gawler Craton below the cover sequences of the Stuart Shelf (Fig. 13). Isotopic ages for the breccias are available only for Olympic Dam (1593 ± 7 Ma, U–Pb_{zircon} age; Johnson and Cross, 1991), although in many places iron oxide alteration overprints Hiltaba Suite granites (1585–1595 Ma; Creaser, 1995). With the exception of the mine development at Olympic Dam, the location and extent of breccia complexes is only known from limited drilling under deep sedimentary cover, and from geophysical inferences. The breccias are part of a more extensive hydrothermal spectrum that includes regional disseminated iron oxides, sericite, and chlorite, and local magnetite–hematite ± calc–silicate skarn replacement zones (Paterson et al., 1986). Intense zones of iron-oxide ± Cu–U–Au–Co–REE mineralization (including at least 30 named systems) are confined to a 200 × 100 km NW-trending ellipse in the central Olympic Subdomain (Fig. 13), which is in turn part of a much larger magmatic province comprising the Gawler Range Volcanics and the plutons of the Hiltaba Suite (Creaser, 1995; Daly et al., 1998). Breccias and massive iron oxide zones are mainly absent from the rest of the province. At least seven of the documented mineralized systems include major hydrothermal breccia complexes (Olympic Dam, Wirrda Well, Acropolis, Oak Dam, Snake Gully, Emmie Bluff, and Winjabbie; Hinde, 1982; Paterson et al., 1986; Cross, 1993; Cross et al., 1993; Davidson and Patterson, 1993; Gow et al., 1993; Daly et al., 1998), as well as many other sites with subordinate breccias. In addition to hydrothermal varieties, there are small volumes of the following breccia types at different sites: fault breccias, corrosion breccias, autobrecciated and peperitised

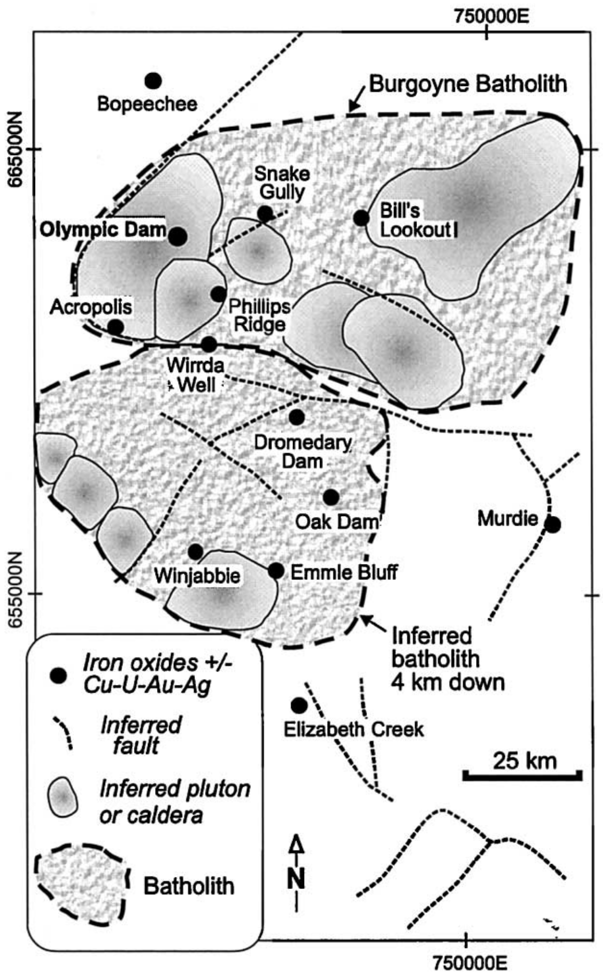

Fig. 13. An interpretation of the geophysical data and prospect locations from the Olympic Subdomain, South Australia, after Gow et al. (1993), combined with the Burgoyne Batholith concept of Reeve et al. (1990). Approximate location is indicated by the position of the Olympic Dam breccia in Fig. 14.

dikes, and sedimentary breccias (mainly consisting of reworked hydrothermal breccia).

Nearly identical ages and similarities in metallogeny make correlation of the Wernecke and Stuart Shelf breccia complexes attractive. However, a definite connection between the two complexes is inhibited by the lack of Stuart Shelf exposure and the absence of detailed petrologic information from the Wernecke Breccias. In order to draw attention to the differences and similarities between the breccia complexes, we provide the following summary of salient features.

A. *Fault relations*. Faulting is an important control on breccia location in both terranes. Gow et al. (1993) interpreted the Stuart Shelf basement to consist of cauldrons, lobate intrusions, and polygonal ring fractures forming a NW- and NE-trending fault mesh, on the assumption that iron oxides delineated faults and intrusion margins. Some hydrothermal systems lie on these faults. For instance, the northern arm of the hematite zone at Olympic Dam, and most of its constituent breccia bodies, thickened high-grade ore intercepts, and mafic-ultramafic dikes, are elongate parallel to local late strike–slip faults (Sugden and Cross, 1991), which parallel the regional NW-trending fault fabric (Reeve et al., 1990). Some breccia complexes (e.g., Oak Dam and Emmie Bluff) and massive mineralization with minor breccia (e.g., Murdie), are elongate parallel to recognized fault directions (Paterson, 1988; Gow et al., 1994).

B. *Wallrock relations*. Breccias at both sites are dominated by the immediate wallrock lithologies, with minor representation of rocks above and below the level of exposure. On the Stuart Shelf these not only include volcano-plutonic elements, but older deformed Lincoln Complex granites (e.g., Wirrda Well), Hutchison Group (e.g., Oak Dam), and Wandearah Metasiltstone (e.g., Emmie Bluff). The gradational contact relations associated with some Wernecke bodies apply to most Stuart Shelf examples.

C. *Scale*. Similar restricted scales of brecciation occur in each district. The Olympic Subdomain has an area of $\sim 15\,700$ km^2, compared to $\sim 48\,000$ km^2 for the Wernecke Breccias; both occupy only small fractions of their host provinces. Olympic Dam is the largest single zone in the Olympic Subdomain (7×5 km), but more typical bodies measure 1.0×0.3 km (e.g., Oak Dam East), comparable to many Wernecke Breccia zones, but smaller than some.

D. *Regional alteration*. Disseminated iron oxide and phyllic alteration is very widespread in the Olympic Subdomain, but alteration and mineralization are generally confined to the environs of Wernecke Breccia zones in Yukon.

E. *Multiple breccias and reworking*. The largest examples from the Olympic Subdomain consist of numerous individual breccia bodies measuring 100×10 of meters. It is not clear that Wernecke bodies are composite features, although multiple stages of hydrothermal activity are locally evident. Olympic Subdomain systems display reworking of previous hydrothermal products, such as massive hematite and siderite clasts mixed with wallrock clasts. All clast types are pervasively metasomatised towards the centers of systems, forming massive hematite–quartz (e.g., Olympic Dam, Oak Dam), and siderite (e.g., Wirrda Well). Wernecke Breccia systems appear to have had less complex histories, characterized by lower fluid fluxes compared to the Stuart Shelf examples, and perhaps less explosive interaction with groundwater.

F. *Syn-breccia magmatism*. Altered felsic to ultramafic peperitic dikes (Krcmarov, 1987) and diatremes (Olympic Dam, Oak Dam) record small-volume mafic magmatic activity concurrent with Olympic Subdomain brecciation. These igneous features are superimposed on a slightly older (ca. 1590 Ma) and more extensive magmatic assemblage comprising the Gawler Range Volcanics and the Hiltaba Suite granites (Creaser, 1995). In the Yukon, the Wernecke Breccias were emplaced into a predominantly sedimentary upper crustal assemblage. No igneous rocks of syn-breccia age are known within the upper crust in this region, although limited isotopic evidence suggests that such rocks may have been emplaced at greater depths.

G. *Crustal level of brecciation*. Resedimented graded breccias, airfall tuff, boiling zones, open-space fill textures, flaring breccia bounding surfaces, dominant phyllic alteration, and even chemical sedimentation are all evidence that

Olympic Subdomain breccias were emplaced at shallow crustal levels, in places venting to the surface to form crater complexes. In the Wernecke Breccias, variable crustal levels are suggested by differences in alteration mineral assemblages. Vent areas are nowhere preserved, but this is probably a function of erosion depth. The presence of > 10 m megaclasts, and in particular the huge, foundered block of the Slab volcanics, suggests that near-surface facies are preserved in some of the breccia zones.

5. Discussion

Similarities in age and petrologic character between the Wernecke Breccias and those in the Olympic Subdomain of the Gawler Craton in South Australia make correlations between the two regions attractive. Correlation between the Olympic Dam and Wernecke breccia zones was suggested by Bell (1982), but this notion was subsequently discounted by the 1.27 Ga age of hydrothermal monazite in one of the Wernecke Breccia zones (Parrish and Bell, 1987). However, the age determinations and field relations described in this paper demonstrate that 1.27 Ga was a time of localized hydrothermal reactivation of Wernecke Breccia, and that the age of voluminous Wernecke brecciation and metasomatism is more compatible with our new U–$Pb_{titanite}$ date of 1.6 Ga. With this finding, correlation between the Wernecke Breccias and the coeval breccias in South Australia is once again viable and compelling.

Detailed and convincing correlation between Late Mesoproterozoic and Neoproterozoic strata in northwestern Canada and southeastern Australia by Eisbacher (1985), Bell and Jefferson (1987), Young (1992) and Rainbird et al. (1996) complement the hypothesis of a common origin for the Australian and Canadian breccias. Paleoproterozoic and early Mesoproterozoic rocks, in contrast, have not been comprehensively correlated, and this topic remains an outstanding vehicle for clarifying the configuration and evolution of the Proterozoic supercontinent known most commonly as Rodinia.

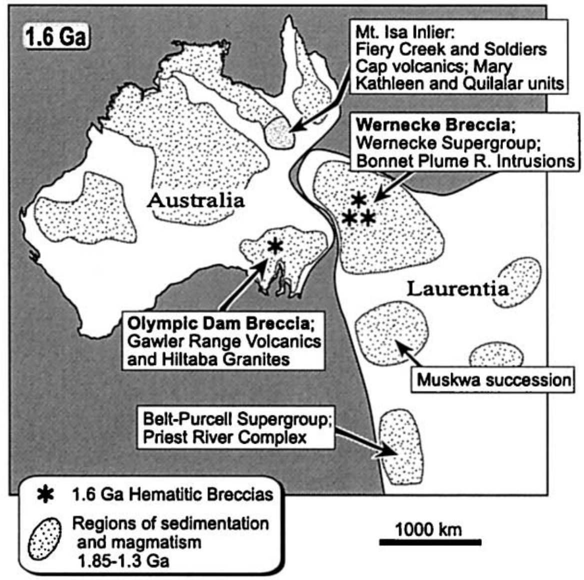

Fig. 14. Continental reconstruction of Australia and Laurasia at 1.6 Ga (after Moores, 1991), showing positions of Wernecke Breccia, the Olympic Dam breccia, and other relevant features. Shape of conjugate coastlines taken from Karlstrom et al. (1999) and Burrett and Berry (2000). Antarctica (not shown) is generally thought to have lain alongside Laurentia, in contact with southern Australia (e.g., Moores, 1991).

A general but robust similarity in terms of basement-cover relations can be drawn between northern Laurentia and Australia, despite the limitations imposed by modest exposure and the effects of Phanerozoic orogenesis. As noted by Hoffman (1989) and Solomon and Groves (1994), both regions were strongly affected by collisional orogenesis and magmatism from ca. 2.0 to 1.84 Ga (Burramundi Orogeny in Australia, and Wopmay-Great Bear-Fort Simpson orogenesis in Laurentia). Following these events of cratonization, both continental regions underwent episodes of widespread basin formation, continental magmatism, and contraction later in Proterozoic time (Fig. 14). In Yukon, for example, cover sequences of predominantly sedimentary character were deposited at > 1.71 Ga (Wernecke Supergroup), and approximately 1.38, 1.0 and 0.7 Ga (Eisbacher, 1981; Ross, 1991; Abbott et al., 1997; Thorkelson, 2000).

We identify two possible cross-continental linkages involving late Paleoproterozoic rocks of similar age and composition (Fig. 14). Firstly, the Quilalar Formation and the Mary Kathleen Group of the Mt. Isa Inlier (Blake, 1987) are proposed as sedimentary equivalents of the Wernecke Supergroup. Secondly, the Fiery Creek Volcanics (Page and Sun, 1998) and related intrusions of the Mt. Isa Inlier of Australia are suggested as possible correlatives of the 1.71 Ga Bonnet Plume River intrusions. As illustrated in Fig. 14, the Mt. Isa and Yukon regions may have lain close to one another in Paleo- to Mesoproterozoic time. Although contiguity cannot be firmly demonstrated, the suggested sedimentary and igneous linkages between Yukon and the Mt. Isa inlier, plus the more compelling correlation between hematitic breccias in Yukon and the Gawler region, provide a reasonable basis for the continental configuration proposed in Fig. 14. These connections are consistent with the configurations of Bell and Jefferson (1987), Moores (1991), and the global reconstructions of Young (1992, 1995), all of which place South Australia close to northwestern Canada.

One difficulty in restoring South Australia next to Yukon is the apparent success of models which place South Australia next to southwestern Canada or the western United States (e.g., Dalziel, 1991; Ross et al., 1992; Idnurm and Giddings, 1995; Doughty et al., 1998; Karlstrom et al., 1999, this volume; Burrett and Berry, 2000). Each of these models relies on a different set of proposed correlations, and none of the models take into account all of the possible linkages. For example, Doughty et al. (1998) made a strong argument for placing South Australia next to the northwestern United States, based almost entirely on correlations between the ca. 1.6 Ga Gawler Range volcanics and the Hiltaba Suite granites of South Australia, and the slightly younger igneous rocks of the Priest River Complex (Fig. 14). The configurations of Karlstrom et al. (1999), this volume) and Burrett and Berry (2000), which place Australia against the southwestern United States, are based on a wider range of data, but do not substantively address the possible correlations between units in Australia and northern Laurentia. Thus, the efficacy of each of the models is subjective, leaving the configuration proposed in Fig. 14 as a viable option for part of the Rodinian mosaic at the time of Wernecke Breccia genesis.

If South Australia lay next to northwestern Laurentia at ca. 1.6 Ga (Fig. 14), then the breccia fields of both continents could constititute a single hydrothermal province of enormous size, ≈ 1000 km in diameter. This province of Australian-Laurentian brecciation could be explained by the arrival of a large mantle plume head at 1.6 Ga, giving rise to regional heating of the continental lithosphere. In the Yukon, heating may have been sufficient to drive metamorphic dehydration and modest magmatism, leading to voluminous hydrothermal activity in the upper crust. In South Australia, a higher thermal flux and more voluminous mantle-derived magmatism may have led to crustal melting and anorogenic felsic magmatism (Creaser, 1995) with accompanying hydrothermal activity.

Acknowledgements

Funding was provided by the governments of Canada and Yukon Territory, the SNORCLE transect of Lithoprobe, and the Natural Sciences and Engineering Council of Canada. Logistical support by the Newmont-Westmin-Pamicon-Equity joint venture, and by BHP Minerals, increased the effectiveness of the field program. Western Mining Corporation is thanked for access to data and samples. GJD was funded by the Australian Research Council fellowship scheme. Carol Wallace provided excellent research assistance. C. Jefferson and D. Long provided insightful reviews. This paper is a contribution to the International Geological Correlation Program, Projects 400 and 440, and to Lithoprobe (pub. no. 1154).

References

Abbott, J.G., 1997. Geology of the upper Hart River Area, Eastern Ogilvie Mountains, Yukon Territory (116A/10. 116A/11). Exploration and Geological Services Division, Yukon, Indian and Northern Affairs Canada Bull. 9, p. 76.

Abbott, G., Thorkelson, D., Creaser, R. Bevier, M.L., Mortensen, J., 1997. New correlations among Proterozoic successions and intrusive breccias in the Ogilvie and Wernecke Mountains, Yukon. In: Cook, F., Erdmer, P. (Compilers), Slave-Northern Cordillera Lithospheric Evolution (SNORCLE) Transect and Cordilleran Tectonics Workshop Meeting (March 7–9), University of Calgary, Lithoprobe Rept., 56: 188–197.

Aitken, J.D., McMechan, M.E., 1992. Middle Proterozoic assemblages, Chapter 5. In: Gabrielse, H., Yorath, C.J. (Eds.), Geology of the Cordilleran Orogen in Canada. Geol. Surv. Can, pp. 97–124.

Archer, A., Bell, R.T., Thorpe, R.I., 1986. Age relationships from U-Th-Pb isotope studies of uranium mineralization in Wernecke breccias, Yukon Territory. Current Research, Part A, Geol. Surv. Can. Pap. 86 (1A), 385–391.

Archer, A., Schmidt, U., 1978. Mineralized breccias of early Proterozoic age, Bonnet Plume River district, Yukon Territory. Can. Min. Met. Bull. 71, 53–58.

Bell, R.T., 1968. Proterozoic stratigraphy of northeastern British Columbia. Geol. Surv. Can. Pap. 67–68, 75.

Bell, R.T., 1982. Comments on the geology and uraniferous mineral occurrences of the Wernecke Mountains, Yukon and District of Mackenzie. Current Research, Part B, Geol. Surv. Can. Pap. 82 (1B), 279–284.

Bell, R.T., 1986a. Geological map of northeastern Wernecke Mountains, Yukon Territory. Geol. Surv. Can. Open File 1207.

Bell, R.T., 1986b. Megabreccias in northeastern Wernecke Mountains, Yukon Territory. Current Research, Part A, Geol. Surv. Can. Pap. 1986–1A, 375–384.

Bell, R.T., 1989. A conceptual model for development of megabreccias and associated mineral deposits in Wernecke Mountains, Canada, Copperbelt, Zaire, and Flinders Range, Australia. In: Uranium resources and geology of North America, Proc. technical committee meeting organized by the International Atomic Energy Agency and held in Saskatoon, Canada, Sept. 1–3, 1987. International Atomic Energy Agency, Vienna, pp. 149–169.

Bell, R.T., Delaney, G.D., 1977. Geology of some uranium occurrences in Yukon Territory. Current Research, Part A, Geol. Surv. Can. Pap. 77–1A, 33–37.

Bell, R.T., Jefferson, C.W., 1987. A hypothesis for an Australian-Canadian connection in the late Proterozoic and the birth of the Pacific Ocean. In: Proc. Pacific Rim Congr. 87, Parkville, Victoria, Australia. Australasian Institute of Mining and Metallurgy, pp. 39–50.

Blake, D.H., 1987. Geology of the Mount Isa Inlier and environs, Queensland and Northern Territory. Bureau of Mineral Resources Bull. 225, 83.

Burrett, C., Berry, R., 2000. Proterozoic Australia-Western United States (AUSWUS) fit between Laurentia and Australia. Geology 28, 103–106.

Conly, A.G., 1993. Mineralogy and mineral chemistry of hydrothermal alteration of Wernecke Breccia from the Slats Creek (NTS 106D/16) map area, Wernecke Mountains, Yukon. Unpublished Report, Carleton University, Ottawa, p. 60.

Conly, A.G., Taylor, R.P., Thorkelson, D.J., Fallick, A.E., 1995. Petrography, mineralogy, and stable isotope geochemistry of hydrothermal alteration of Wernecke Breccia, Slats Creek area, Yukon Territory. Geol. Assoc. Can. Prog. Abstr. 20, A–116.

Cook, F.A., 1992. Racklan Orogen. Can. J. Earth Sci. 29, 2490–2496.

Cook, F.A., van der Velden, A.J., Hall, K.W., Roberts, B.J., 1998. Tectonic Delamination of the Precambrian Lithosphere in Northwestern Canada Mapped by LITHOPROBE. Lithoprobe Rept. 64, 58–69.

Creaser, R.A., 1995. Neodymium isotopic constraints for the origin of Mesoproterozoic felsic magmatism, Gawler Craton, South Australia. Can. J. Earth Sci. 32, 460–471.

Cross, K.C., 1993. Mineralisation associated with the Gawler Range Volcanics and Hiltaba Suite granitoids: Acropolis and Wirrda Well deposits. In: Drexel, J.F., Preiss, W.V., Parker, A.J. (Eds.), The Geology of South Australia. South Australian Geological Survey, Bull. 54: 138

Cross, K.C., Daly, S.J., Flint, R.B., 1993. Mineralisation associated with the Gawler Range Volcanics and Hiltaba Suite granitoids: Olympic Dam deposit. In: Drexel, J.F., Preiss, W.V., Parker, A.J. (Eds.), The Geology of South Australia. South Australian Geological Survey, Bull. 54: 132–138.

Daly, S.J., Fanning, C.M., Fairclough, M.C., 1998. Tectonic evolution and exploration potential of the Gawler Craton, South Australia. AGSO J. Aust. Geol. Geophys. 17, 145–168.

Dalziel, I.W.D., 1991. Pacific margins of Laurentia and East Antarctica–Australia as a conjugate rift pair: evidence and implications for an Eocambrian supercontinent. Geology 19, 598–601.

Davidson, G.J., Patterson, H.L., 1993. Oak Dam East: a prodigious, uranium-bearing, massive iron-oxide body on the Stuart Shelf. Geological Society of Australia 34, 18–19 Abstr.

Delaney, G.D., 1981. The Mid-Proterozoic Wernecke Supergroup, Wernecke Mountains, Yukon Territory. In: Campbell, F.H.A. (Ed.), Proterozoic Basins of Canada, Geol. Surv. Can. Pap. 81–10, p. 23.

Doughty, P.T., Price, R.A., Parrish, R.R., 1998. Geology and U–Pb geochronology of Archean basement and Proterozoic cover in the Priest River complex, northwestern United States, and their implications for Cordilleran structure and Precambrian continent reconstructions. Can. J. Earth Sci. 35, 39–54.

Dredge Mitchelmore, M., Cook, F.A., 1994. Inversion of the Proterozoic Wernecke basin during tectonic development of the Racklan Orogen, northwest Canada. Can. J. Earth Sci. 31, 447–457.

Eisbacher, G.H., 1981. Sedimentary tectonics and glacial record in the Windermere Supergroup, Mackenzie Mountains, northwestern Canada. Geol. Surv. Can. Pap. 80–27.

Eisbacher, G.H., 1985. Late Proterozoic rifting, glacial sedimentation, and sedimentary cycles in the light of Windermere deposition, western Canada. Palaeogeograph. Palaeoclimatol. Palaeoecol. 51, 231–254.

Francis, D., 1994. Chemical interaction between picritic magmas and upper crust along the margins of the Muskox intrusion, Northwest Territories. Geol. Surv. Can. Pap. 92–12, p. 94.

Gabrielse, H., 1967. Tectonic evolution of the northern Canadian Cordillera. Can. J. Earth Sci. 4, 271–298.

Gandhi, S.S., Bell, R.T., 1990. Metallogenic concepts to aid exploration for the giant Olympic Dam-type deposits and their possible derivatives. In: Proceedings of the Eighth Quadrennial IAGOD Symposium, Ottawa, Canada, 1990, pp. 787–802.

Gow, P.A., Wall, V.J., Valenta, R.K., 1993. The regional geophysical response of the Stuart Shelf, South Australia. Exploration Geophysics 24, 513–520.

Gow, P.A., Wall, V.J., Oliver, N.H.S., Valenta, R.K., 1994. Proterozoic iron oxide (Cu-U-Au-REE) deposits: further evidence of hydrothermal origins. Geology 22, 633–636.

Green, L.H., 1972. Geology of Nash Creek, Larsen Creek, and Dawson Creek map-areas, Yukon Territory. Geol. Surv. Can. 364, 157 Mem.

Hinde, J.S., 1982. A study of the relationships between the mean element abundances of the Stuart Shelf and Olympic Dam basement lithologies, relative to felsic and mafic rocks. Unpublished Western Mining Report, SS1–1, p. 15.

Hitzman, M.W., Oreskes, N., Einaudi, M.T., 1992. Geological characteristics and tectonic setting of Proterozoic iron oxide (Cu-U-Au-REE) deposits. In: Gall, G., Schulz, K. (Eds.), Precambrian Metallogeny Related to Plate Tectonics. Precambrian Res. 58: 241–287.

Hoffman, P.F., 1989. Precambrian geology and tectonic history of North America. In: Bally, A.W., Palmer, A.R. (Eds.), The Geology of North America – an overview, Geology of North America, A. Geol. Soc. Am. Boulder, pp. 447–512.

Idnurm, M., Giddings, J.W., 1995. Paleoproterozoic-Neoproterozoic North America-Australia link: new evidence from paleomagnetism. Geology 23, 149–152.

INAC, 1998. Yukon Minfile. Exploration and Geological Services Division, Yukon, Indian and Northern Affairs, Canada, map areas 106C, 106D.

Jefferson, C.W., Parrish, R.R., 1989. Late Proterozoic stratigraphy, U–Pb zircon ages, and rift tectonics, Mackenzie Mountains, northwestern Canada. Can. J. Earth Sci. 26, 1784–1801.

Johnson, J.P., Cross, K.C., 1991. Geochronological and Sm-Nd isotopic constraints on the genesis of the Olympic Dam Cu-U-Au-Ag deposit, South Australia. In: Pagel, M., Leroy, J.L. (Eds.), Source, transport and deposition of metals. Proceedings of the 25 years SGA anniversary meeting. Balkema, Rotterdam, pp. 395–400.

Karlstrom, K.E., Harlan, S.S., Williams, M.L., McLelland, J., Geissman, J.W., Ahall, K.-I., 1999. Refining Rodinia: geological evidence for the Australia-Western U.S. connection in the Proterozoic. GSA Today 9 (10), 1–6.

Krcmarov, R., 1987. The geology, petrology and geochemistry of the volcanic unit at Olympic Dam, South Australia. Unpublished honours thesis, Univ. of Adelaide.

Lane, R.A., 1990. Geologic setting and petrology of the Proterozoic Ogilvie Mountains Breccia of the Coal Creek inlier, southern Ogilvie Mountains, Yukon Territory. MSc thesis, Univ. of British Columbia, Vancouver, Canada, p. 223.

Laznicka, P., Edwards, R.J., 1979. Dolores Creek, Yukon – a disseminated copper mineralization in sodic metasomatites. Econ. Geol. 74, 1352–1370.

Laznicka, P., Gaboury, D., 1988. Wernecke breccias and Fe, Cu, U mineralization: Quartet Mountain-Igor area (NTS 106E). In: Yukon Geology, v. 2. Exploration and Geological Services Division, Yukon, Indian and Northern Affairs Canada, pp. 42–50.

LeCheminant, A.N., Heaman, L.M., 1989. Mackenzie igneous events, Canada: middle Proterozoic hotspot magmatism associated with ocean opening. Earth Planet. Sci. Lett. 96, 38–48.

Long, D.G.F., Devaney, J.R., Pratt, B.R., 1999. Tectonostratigraphic framework of the Mesoproterozoic Muskwa assemblage, northern British Columbia. In: Cook, F., Erdmer, P. (Compilers), Slave-Northern Cordilleran Cordilleran Lithospheric Evolution (SNORCLE) Transect and Cordilleran Tectonics Workshop Meeting, University of Calgary, Lithoprobe Rept. 69: 112–119.

Ludwig, K.R., 1998. Isoplot/Ex, a geochronological toolkit for Microsoft Excel, version 1.00b: Berkeley Geochronology Center, Special Publication No. 1.

Mitchell, R.H., 1991. Kimberlites and lamproites: primary sources of diamond. Geosci. Canada 18, 1–16.

Moores, E.M., 1991. Southwest U.S.-East Antarctic (SWEAT) connnection: a hypothesis. Geology 19, 425–428.

Mortensen, J.K., Ghosh, D. Ferri, F., 1995. U–Pb age constraints of intrusive rocks associated with Copper-Gold porphyry deposits in the Canadian Cordillera. In: Schroeter, T.G. (Ed.), Porphyry deposits of the northwestern Cordillera of North America. Canadian Institute of Mining and Metallurgy, Spec. Vol., 46: 142–158.

Norris, D.K., Dyke, L.D., 1997. Chapter 4: Proterozoic. In: Norris, D.K. (Ed.), The Geology, Mineral and Hydrocarbon Potential of Northern Yukon Territory and Northwestern District of Mackenzie. Geol. Surv. Can. Bull. 422: 65–84.

Page, R.W., Sun, S-S., 1998. Aspects of geochronology and crustal evolution in the Eastern Fold Belt, Mt. Isa Inlier. Austr. J. Earth Sci. 45, 343–361.

Parrish, R.R., Bell, R.T., 1987. Age of the NOR breccia pipe, Wernecke Supergroup, Yukon Territory. In: Radiogenic Age and Isotopic Studies: Report 1. Geol. Surv. Can. Pap. 87–2: 39–42.

Parrish, R., Roddick, J.C., Loveridge, W.D., Sullivan, R.W., 1987. Uranium-lead analytical techniques at the geochronology laboratory, Geological Survey of Canada. In: Radiogenic age and isotopic studies, Report 1. Geol. Surv. Can. Pap. 87–2: 3–7.

Paterson, H.L., 1988. Stuart Shelf Joint Venture Oak Dam prospect summary report. Unpublished Western Mining Company report K/3148, p. 14.

Paterson, H.L., Dalgarno, C.R., Esdale, D.J., Tonkin, D., 1986. Basement geology of the Stuart Shelf region, South Australia. In: 8th Australian Geological Convention, Adelaide, 1986. Excursion Guide, vol. A1, pp. 7–12.

Rainbird, R.H., Jefferson, C.W., Young, G.M., 1996. The early Neoproterozoic sedimentary Succession B of northwestern Laurentia: correlations and paleogeographic significance. Geol. Soc. Am. Bull. 108, 454–470.

Reeve, J.S., Cross, K.C., Smith, R.N., Oreskes, N., 1990. Olympic Dam copper-uranium-gold-silver deposit. In: Hughes, F.E., (Ed.), Geology of the mineral deposits of Australia and Papua New Guinea. Australasian Institute of Mining and Metallurgy, Monograph 14: 1009–1035

Roddick, J.C., 1987. Generalized numerical error analysis with application to geochronology and thermodynamics. Geochim. Cosmochim. Acta 51, 2129–2135.

Ross, G.M., 1991. Tectonic setting of the Windermere Supergroup revisited. Geology 19, 1125–1128.

Ross, G.M., Parrish, R.R., Winston, D., 1992. Provenance and U–Pb geochronology of the Mesoproterozoic Belt Supergroup (northwestern United States): implications for age of deposition and pre-Panthalassa plate reconstructions. Earth Planet. Sci. Lett. 113, 57–76.

Solomon, M., Groves, D.I., 1994. The Geology and Origin of Australia's Mineral Deposits. Oxford University Press, New York, p. 951.

Stacey, J.S., Kramer, J.D., 1975. Approximation of terrestrial lead isotope evolution by a two-stage model. Earth Planet. Sci. Lett. 26, 207–221.

Steiger, R.H., Jäger, E., 1977. Subcommission on geochronology: convention on the use of decay constants in geo- and cosmochronology. Earth Planet. Sci. Lett. 36, 359–362.

Sugden, T.J., Cross, K.C.,1991. Significance of overprinting fault systems in the Olympic Dam breccia complex. In: Structural Geology and Exploration. University of Western Australia Geology Department and University Extension Publication 25: 93–98.

Tempelman-Kluit, D.J., 1981. NOR, summary of assessment work and description of mineral properties. In: Yukon Geology and Exploration, 1979-1980. Exploration and Geological Services Division, Yukon, Indian and Northern Affairs Canada, pp. 300–301.

Thorkelson, D.J., 2000. Geology and mineral occurrences of the Slats Creek, Fairchild Lake and "Dolores Creek" areas, Wernecke Mountains (106D/16, 106C/13, 106C/14), Yukon Territory. Exploration and Geological Services Division, Yukon, Indian and Northern Affairs Canada Bull. 10: p. 73

Thorkelson, D.J., Wallace, C.A., 1993. Development of Wernecke breccias in Slats Creek (106D/16) map area, Wernecke Mountains, Yukon. In: Yukon Exploration and Geology, 1992. Exploration and Geological Services Division, Yukon, Indian and Northern Affairs Canada, pp. 19–30.

Thorkelson, D.J., Wallace, C.A., 1995. Geology and mineral occurrences of the "Dolores Creek" map area (106C/14), Wernecke Mountains, northeastern Yukon. In: Yukon Exploration and Geology, 1994. Exploration and Geological Services Division, Yukon, Indian and Northern Affairs Canada, pp. 19–30.

Thorkelson, D.J., Wallace, C.W., 1998a. Geological map of Slats Creek area, Wernecke Mountains, Yukon (106D/16). Indian and Northern Affairs Canada, Exploration and Geological Services Division, Geoscience Map 1998-9, scale 1:50 000.

Thorkelson, D.J., Wallace, C.W., 1998b. Geological map of Fairchild Lake area, Wernecke Mountains, Yukon (106C/13). Indian and Northern Affairs Canada, Exploration and Geological Services Division, Geoscience Map 1998-10, scale 1:50 000

Thorkelson, D.J., Wallace, C.W., 1998c. Geological map of "Dolores Creek" area, Wernecke Mountains, Yukon (106C/14). Indian and Northern Affairs Canada, Exploration and Geological Services Division, Geoscience Map 1998-11, scale 1:50 000

Thorkelson, D.J., Abbott, J.G., Mortensen, J.K., Creaser, R.A., Villeneuve, M.E., 1998. Proterozoic sedimentation, magmatism, metasomatism and deformation in the Wernecke and Ogilvie Mountains, Yukon. In: Cook, F., Erdmer, P. (Compilers), Slave-Northern Cordillera Lithospheric Evolution (SNORCLE) Transect and Cordilleran Tectonics Workshop Meeting (March 6–8), Simon Fraser University, Lithoprobe Report No. 64, pp. 110–119.

Villeneuve, M.E., Theriault, R.J., Ross, G.M., 1991. U–Pb ages and Sm-Nd signature of two subsurface granites from the Fort Simpson magnetic high, northwest Canada. Can. J. Earth Sci. 28, 1003–1008.

Wheeler, J.O., McFeely, P., 1991. Tectonic assemblage map of the Canadian Cordillera and adjacent parts of the United States of America. Geol. Surv. Can., Map 1712A, scale 1:2 000 000.

Yamashita, K., Creaser, R.A., Jensen, J.E., Heaman, L.M., 2000. Origin and evolution of mid-to late-Archean crust in the Hanikahimajuk Lake area, Slave Province, Canada; Evidence from U–Pb geochronological, geochemical and Nd-Pb isotopic data. Precam. Res. 99, 197–224.

Young, G.M., 1992. Late Proterozoic stratigraphy and the Canada-Australian connection. Geology 20, 215–218.

Young, G.M., 1995. Are Neoproterozoic glacial deposits preserved on the margins of Laurentia related to the fragmentation of two supercontinents? Geology 23, 153–156.